

# Supporting Information

## Popular C<sub>82</sub> Cage Encapsulating a Divalent Metal Ion Sm<sup>2+</sup>: Structure and Electrochemistry

*Ziqi Hu,<sup>a</sup> Yajuan Hao,<sup>b</sup> Zdeněk Slanina,<sup>c</sup> Zhenggen Gu,<sup>b</sup> Zujin Shi,<sup>\*a</sup> Filip Uhlík,<sup>d</sup> Yunfeng Zhao,<sup>b</sup> Lai Feng<sup>\*b</sup>*

<sup>a</sup>Beijing National Laboratory for Molecular Sciences, State Key Lab of Rare Earth Materials Chemistry and Applications, College of Chemistry and Molecular Engineering, Peking University, Beijing 100871, China;

<sup>b</sup>College of Physics, Optoelectronics and Energy & Collaborative Innovation Center of Suzhou Nano Science and Technology, Soochow University, Suzhou 215006, China

<sup>c</sup>Life Science Center of Tsukuba Advanced Research Alliance, University of Tsukuba, Tsukuba 305-8577, Japan

<sup>d</sup>Department of Physical and Macromolecular Chemistry, Faculty of Science, Charles University in Prague, Albertov 6, 128 43 Praha 2, Czech Republic

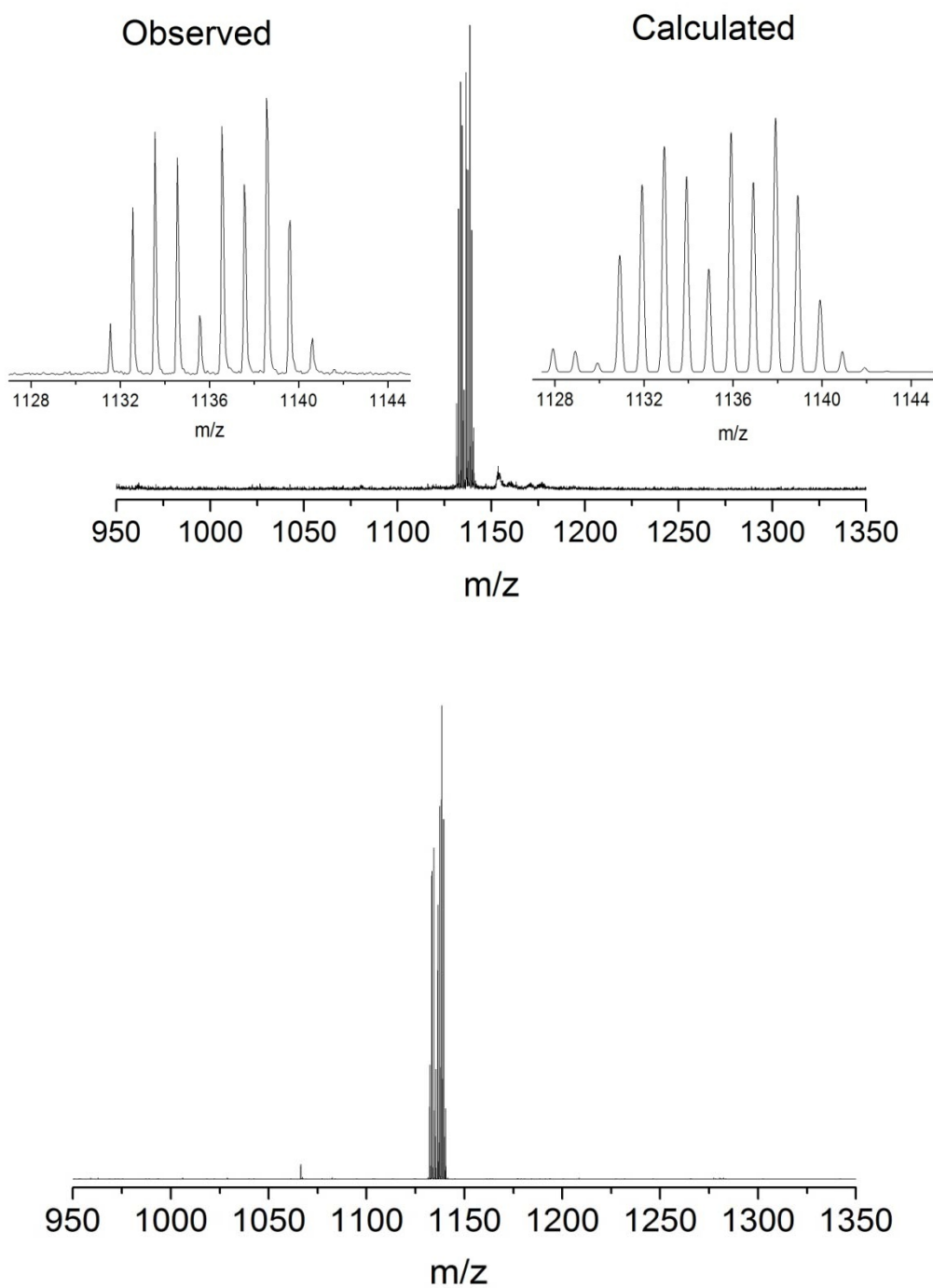


**Figure S1.** MALDI-TOF mass spectra of the purified samples of  $\text{Sm}@C_{2v}(9)\text{-C}_{82}$  (up) and  $\text{Sm}@C_{3v}(7)\text{-C}_{82}$  (down) in positive-ion reflection mode. The insets show the observed and calculated isotopic distributions of  $\text{Sm}@C_{82}$ .

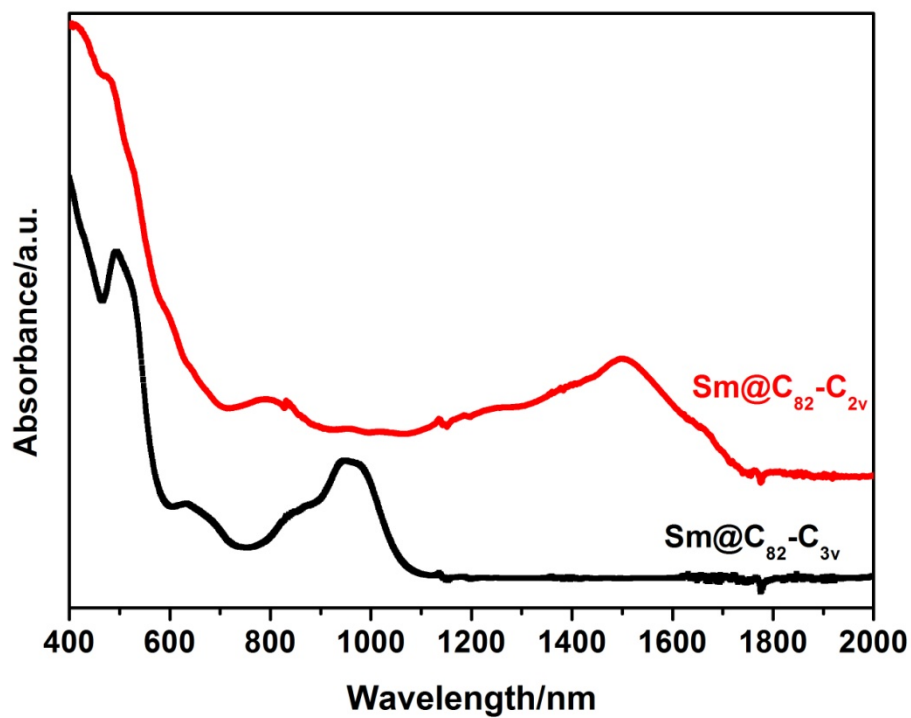


**Figure S2.** UV-vis-NIR absorption spectra of Sm@C<sub>2v</sub>(9)-C<sub>82</sub> (red) and Sm@C<sub>3v</sub>(7)-C<sub>82</sub> (black) in toluene solution. Particularly, the absorption characteristics of Sm@C<sub>3v</sub>(7)-C<sub>82</sub> are very similar to that of Ca@C<sub>82</sub>(II). (see Ref: *J. Am. Chem. Soc.*, 1996, 118, 11309-11310.)

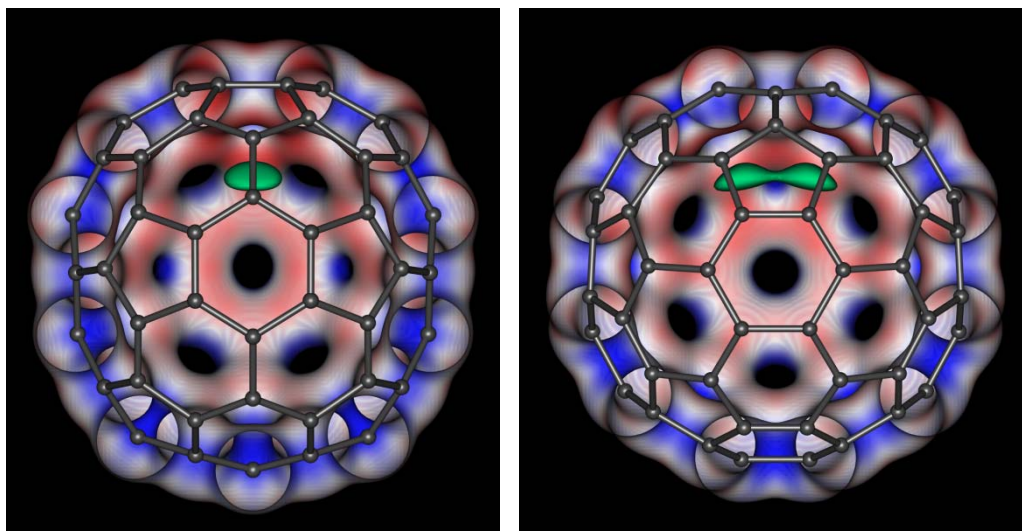


**Figure S3.** Two orthogonal views of the M06-2X/3-21G electrostatic potential (ESP) in  $C_{2v}-(C_{82})^{2-}$ , namely of its -144 kcal/mol isoenergetic surface (in green), moreover superimposed with a cross-section of the charge-density  $0.05e/\text{Bohr}^3$  contour on which the ESP values are indicated by red (-63), white (0) and blue (+63 kcal/mol). Either of the two ESP minima has energy of -145.4 kcal/mol. In the left panel, the cage orientation is set to be identical to those shown in Figures S5.

Note: *Figure S3* shows that there are actually two minima symmetrically placed along the symmetry axis (the distance between those two ESP minima is  $1.50 \text{ \AA}$ ). Still, the potential is shallow-the energy within the green cloud is already nearly constant. As for the distance, each of the two minima has the distance of  $1.94 \text{ \AA}$  from the center of the adjacent hexagon. In Figure S4, the Sm7 site is also under the hexagon with a contact distance of  $2.42 \text{ \AA}$ . However, the distance between the Sm1 site and the hexagon center is  $3.55 \text{ \AA}$ . So, it is obvious that the minor site Sm7 resides more close to the potential minimum as compared to the Sm1 site.

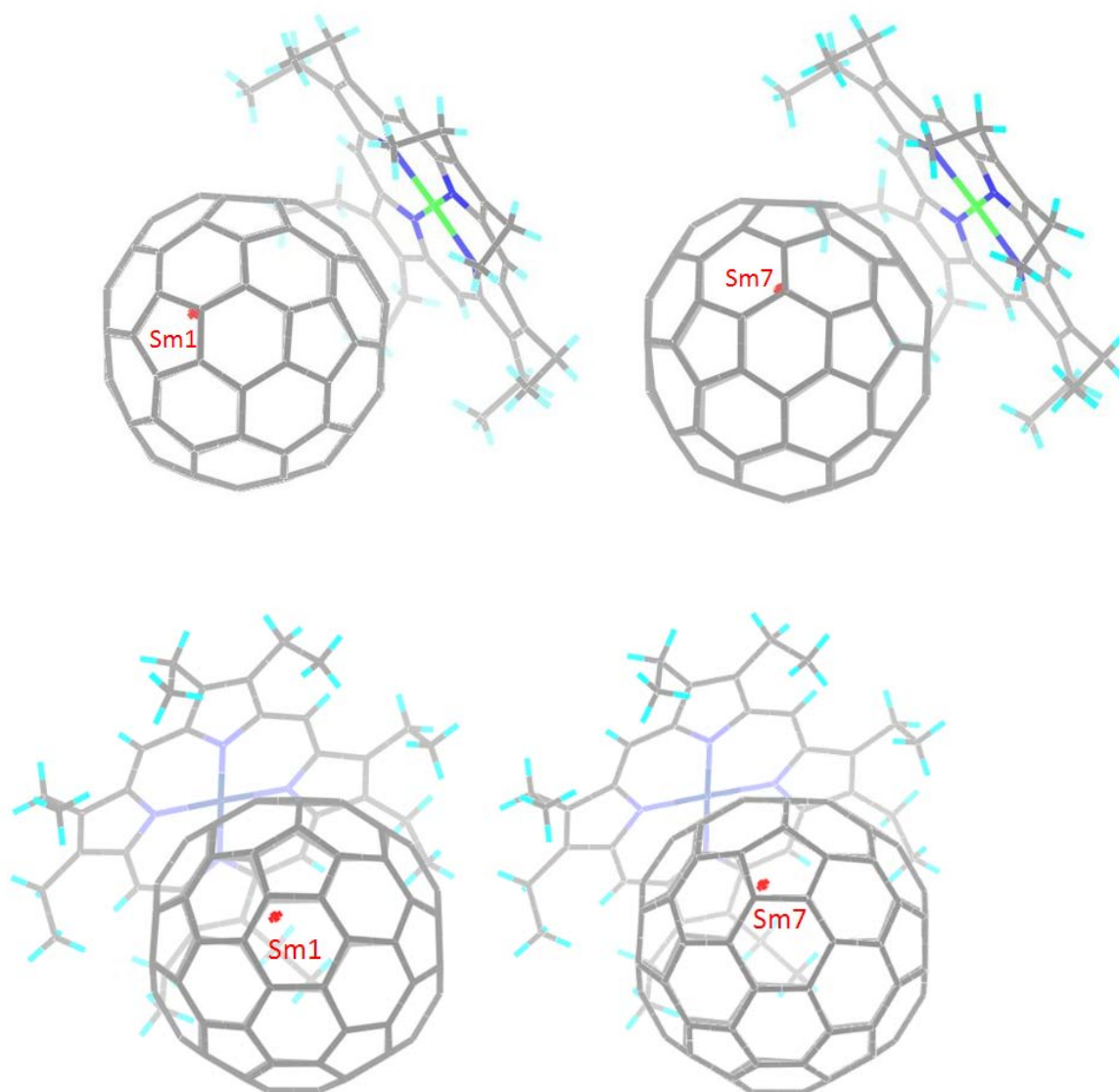


**Figure S4.** Two orthogonal views of the X-ray-determined Sm@C<sub>2v</sub>(9)-C<sub>82</sub>/[Ni<sup>II</sup>(OEP)] models containing major cage orientation along with Sm1 and Sm7 sites, respectively.

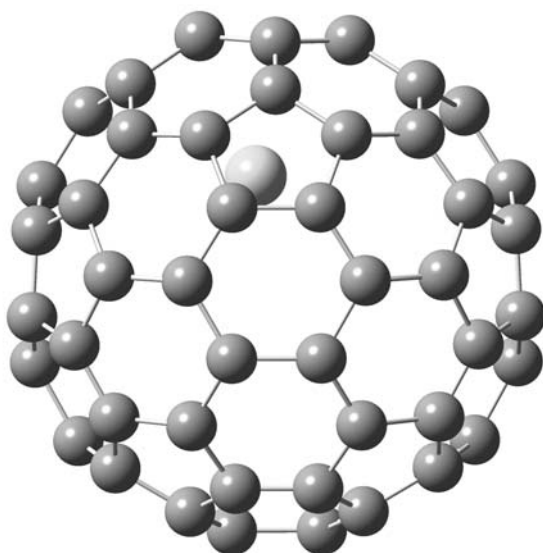


**Figure S5.** Structural view of the DFT-optimized Sm@C<sub>2v</sub>(9)-C<sub>82</sub>.

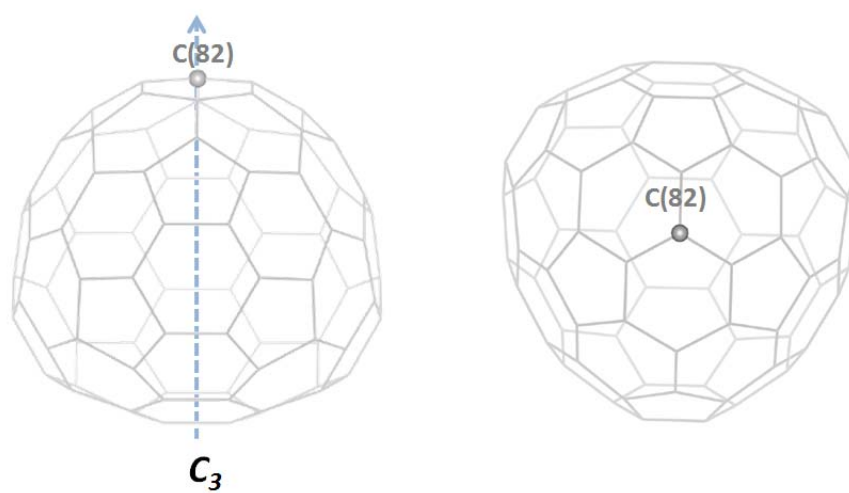


**Figure S6.** Schematic structure of  $C_{3v}(7)-C_{82}$ , showing the position of carbon C(82) and the  $C_3$  axis that passes through the C(82).

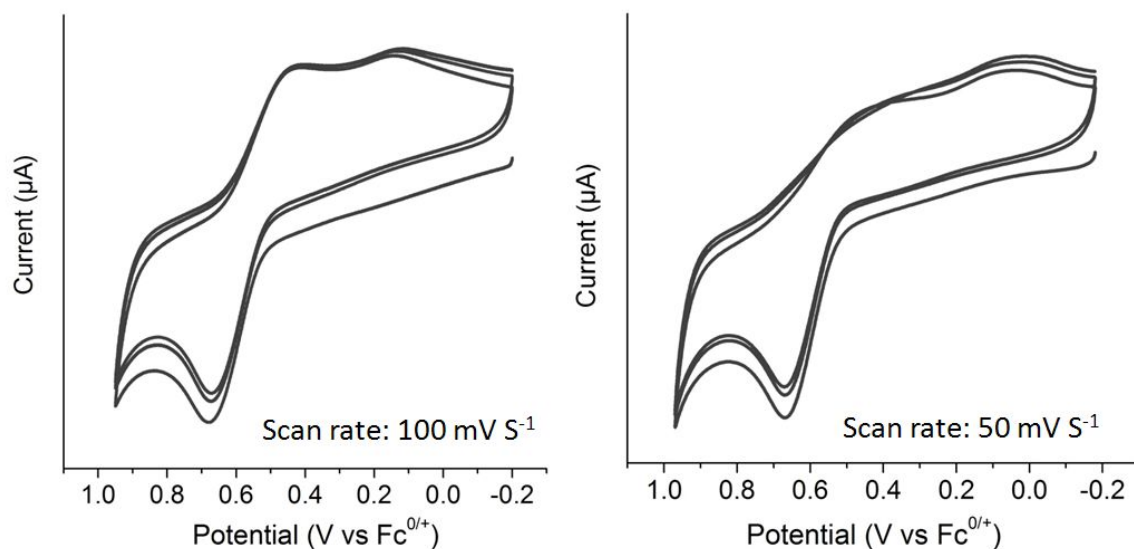


**Figure S7.** Cyclic voltammograms of Sm@C<sub>3v</sub>(7)-C<sub>82</sub> in o-dichlorobenzene containing 0.05 M (n-Bu)<sub>4</sub>NPF<sub>6</sub>, showing the first oxidation step with different scan rate: 100 mV s<sup>-1</sup> (left) and 50 mV s<sup>-1</sup> (right), respectively.

Complete reference 20.

20. M. J. Frisch, G. W. Trucks, H. B. Schlegel, G. E. Scuseria, M. A. Robb, J. R. Cheeseman, G. Scalmani, V. Barone, B. Mennucci, G. A. Petersson, H. Nakatsuji, M. Caricato, X. Li, H. P. Hratchian, A. F. Izmaylov, J. Bloino, G. Zheng, J. L. Sonnenberg, M. Hada, M. Ehara, K. Toyota, R. Fukuda, J. Hasegawa, M. Ishida, T. Nakajima, Y. Honda, O. Kitao, H. Nakai, T. Vreven, J. A. Montgomery, Jr., J. E. Peralta, F. Ogliaro, M. Bearpark, J. J. Heyd, E. Brothers, K. N. Kudin, V. N. Staroverov, R. Kobayashi, J. Normand, K. Raghavachari, A. Rendell, J. C. Burant, S. S. Iyengar, J. Tomasi, M. Cossi, N. Rega, J. M. Millam, M. Klene, J. E. Knox, J. B. Cross, V. Bakken, C. Adamo, J. Jaramillo, R. Gomperts, R. E. Stratmann, O. Yazyev, A. J. Austin, R. Cammi, C. Pomelli, J. W. Ochterski, R. L. Martin, K. Morokuma, V. G. Zakrzewski, G. A. Voth, P. Salvador, J. J. Dannenberg, S. Dapprich, A. D. Daniels, O. Farkas, J. B. Foresman, J. V. Ortiz, J. Cioslowski and D. J. Fox, Gaussian 09, Revision A.02, Gaussian, Inc., Wallingford, CT, 2009.